

Volumetric and Isentropic Compressibility Behavior of Ionic Liquid, 1-Propyl-3-Methylimidazolium Bromide in Acetonitrile, Dimethylformamide, and Dimethylsulfoxide at $T = (288.15 \text{ to } 308.15) \text{ K}$

Rahmat Sadeghi · Hemayat Shekaari ·
Rahim Hosseini

Received: 22 August 2008 / Accepted: 28 August 2009 / Published online: 22 September 2009
© Springer Science+Business Media, LLC 2009

Abstract Density and speed-of-sound data for 1-propyl-3-methylimidazolium bromide ($[\text{C}_3\text{mim}][\text{Br}]$) + acetonitrile (MeCN), $[\text{C}_3\text{mim}][\text{Br}]$ + dimethylformamide (DMF), and $[\text{C}_3\text{mim}][\text{Br}]$ + dimethylsulfoxide (DMSO) binary mixtures in the dilute concentration region are reported at $T = (288.15 \text{ to } 308.15) \text{ K}$. From these data, apparent molar volume, isentropic compressibility, excess molar volume, and isentropic compressibility deviation values have been calculated. Negative deviations from the ideal behavior of both molar volume and isentropic compressibility have been observed for all systems investigated in this study. It has been found that deviations from ideal behavior for the $[\text{C}_3\text{mim}][\text{Br}] + \text{MeCN}$ system are larger than those for the $[\text{C}_3\text{mim}][\text{Br}] + \text{DMF}$ system which, in turn, are larger than those for the $[\text{C}_3\text{mim}][\text{Br}] + \text{DMSO}$ system. The results have been interpreted in terms of ion–dipole interactions and structural factors of the ionic liquid and investigated organic solvents.

Keywords Ionic liquids · Isentropic compressibility ·
1-Propyl-3-methylimidazolium bromide · Volumetric properties

1 Introduction

Ionic liquids (ILs) are organic salts that are liquids at temperatures below 373.15 K. They have received considerable attention as alternatives to traditional organic solvents. Due to the interesting physical and chemical properties of ILs, such as negligible vapor pressure, low melting point, a wide liquid range, suitable viscosity, unique

R. Sadeghi (✉) · R. Hosseini
Department of Chemistry, University of Kurdistan, Sanandaj, Iran
e-mail: rahsadeghi@yahoo.com; rsadeghi@uok.ac.ir

H. Shekaari
Department of Chemistry, Faculty of Science, University of Mohaghegh Ardabili, Ardabil, Iran

permittivity, high thermal stability, good solvents for both polar and nonpolar organic and inorganic substances, high electrical conductivity, and wide electrochemical window, they have been widely used as reaction media, separation solvents, and novel electrolytes [1–4]. Despite their importance and interest, a detailed knowledge on the thermodynamic behavior of mixtures of ILs with organic molecular solvents, which is important for the design of any technological processes, is very limited. In recent years, ILs based on the 1-alkyl-3-methylimidazolium cation ($[C_n\text{mim}]^+$) have received much attention [5]. $[C_n\text{mim}]X$ ($X=\text{Cl}$ and Br) compounds can be used for synthesis of ILs with different anions including organic ones [1,3,6–9]. That is why $[C_n\text{mim}]\text{Br}$ together with $[C_n\text{mim}]\text{Cl}$ represent a potential source of numerous ILs, and the study of their thermodynamic properties is of great importance. Thermodynamic parameters such as heat capacities, enthalpies of phase transitions, and surface tensions for a series of pure 1-alkyl-3-methylimidazolium bromide ILs have been reported at various temperatures [10–14].

In solution, the solvation and interactions of the ions or ion-pairs with the solvent determine the unique properties of these systems [15]. The volumetric and acoustic properties of electrolytic and nonelectrolytic solutions have proved particularly informative in elucidating the solute–solute and solute–solvent interactions. In spite of their importance, there is limited information on the thermodynamic properties of 1-alkyl-3-methylimidazolium bromide in aqueous or nonaqueous solutions [16–31]. As a continuation of our previous study [31] on the thermodynamic properties of the 1-alkyl-3-methylimidazolium bromide solutions, we report here new density and speed-of-sound measurements on mixtures of 1-propyl-3-methylimidazolium bromide ($[C_3\text{mim}][\text{Br}]$) with acetonitrile (MeCN), dimethylformamide (DMF), and dimethylsulfoxide (DMSO) over the range of temperature from 288.15 K to 308.15 K at 5 K intervals in the dilute concentration region. The experimental data have been used to obtain apparent molar volume, isentropic compressibility, excess molar volume, and isentropic compressibility deviation values. The chosen solvents, MeCN, DMF, and DMSO, are versatile compounds, especially in their wide range of applicability as solvents in chemical and technological processes and are inexpensive and easily available at high purity. The calculated quantities can be used in a qualitatively or quantitatively way to provide information about molecular structure and the nature of intermolecular forces in these kinds of liquid mixtures [32,33].

2 Experimental

Reagents used were *N*-methylimidazole (>99%), 1-bromopropane (>99%), acetonitrile (GR, >99.8%), toluene (>99%), dimethylsulfoxide (>99.8%), and dimethylformamide (>99.8%) which were purchased from Merck. These reagents were used without further purification. $[C_3\text{mim}][\text{Br}]$ was prepared and purified using a procedure previously described in the literature [34,35]. Briefly, $[C_3\text{mim}][\text{Br}]$ was synthesized by direct alkylation of *N*-methylimidazole with an excess of 1-bromopropane in a round-bottom flask at 353.15 K for 48 h under a nitrogen atmosphere. The crude product was dissolved in acetonitrile and crystallized by adding dropwise to toluene in an ice bath. The product was dried in high vacuum at 333.15 K using a rotary

Table 1 Density d and speed of sound u for pure solvents investigated in this study at $T = 298.15$ K

	MeCN	DMSO	DMF
Density ($\text{g} \cdot \text{cm}^{-3}$)	0.776609 (Exp.)	1.095278 (Exp.)	0.943917 (Exp.)
	0.776533 [36]	1.095271 [36]	0.94392 [41]
	0.776532 [37]	1.09533 [40]	0.94387 [42]
	0.77667 [38]	1.09527 [41]	
Speed of sound ($\text{m} \cdot \text{s}^{-1}$)	1278.77 (Exp.)	1485.21 (Exp.)	1457.81 (Exp.)
	1278.62 [36]	1485.12 [36]	1457.30 [42]
	1280 [39]	1484.51 [41]	
	1283 [40]		

evaporator for at least 4 h at 0.7 kPa. The obtained $[\text{C}_3\text{mim}][\text{Br}]$ has a purity greater than a mass fraction of 0.98, which was used after vacuum desiccated for at least 48 h to remove trace amounts of moisture. The moisture in $[\text{C}_3\text{mim}][\text{Br}]$ was controlled by the Karl Fischer method during the experimental method, and it was found that the water content in $[\text{C}_3\text{mim}][\text{Br}]$ is less than 0.02 mass %. $[\text{C}_3\text{mim}][\text{Br}]$ was analyzed by ^1H NMR (Bruker Av-300) and IR (Buck Scientific) spectra to confirm the absence of any major impurity.

All the solutions were prepared by mass on a Sartorius CP124S balance precise to within $\pm 10^{-4}$ g. The density and speed of sound of the mixtures were measured at different temperatures with a digital vibrating-tube analyzer (Anton Paar DSA 5000, Austria) with proportional temperature control that kept the samples at the working temperature within $\pm 10^{-3}$ K. The apparatus was calibrated with double-distilled, deionized, and degassed water, and dry air at atmospheric pressure according to the instrument catalog. The density and speed of sound can be measured to $\pm 10^{-6}$ $\text{g} \cdot \text{cm}^{-3}$ and $\pm 10^{-2}$ $\text{m} \cdot \text{s}^{-1}$, respectively, under the most favorable conditions. The uncertainties of density and speed-of-sound measurements were 3×10^{-6} $\text{g} \cdot \text{cm}^{-3}$ and 10^{-1} $\text{m} \cdot \text{s}^{-1}$, respectively. During the course of the experiments, the purity of the solvents was checked by comparing density and speed-of-sound results with literature values at 298.15 K as given in Table 1.

3 Results and Discussion

The experimental density (d) and speed-of-sound (u) data for the MeCN(1) + $[\text{C}_3\text{mim}][\text{Br}](2)$, DMF(1) + $[\text{C}_3\text{mim}][\text{Br}](2)$, and DMSO(1) + $[\text{C}_3\text{mim}][\text{Br}](2)$ mixtures, as a function of molality of $[\text{C}_3\text{mim}][\text{Br}]$ at $T = 288.15$ K, 293.15 K, 298.15 K, 303.15 K, and 308.15 K are reported in Table 2. As can be observed, the densities of investigated solutions decrease with increases in temperature and solvent composition. Table 2 also shows that the speed of sound of investigated systems increases with decreases in temperature and solvent composition. The density and speed of sound of methanolic solutions of $[\text{C}_3\text{mim}][\text{Br}]$ have similar behaviors as those observed in this study [31]. Although the density of aqueous solutions of $[\text{C}_3\text{mim}][\text{Br}]$ has similar

Table 2 Experimental density d and speed-of-sound u data for the binary systems [C₃mim][Br] + organic solvents at different temperatures T and ionic liquid molality m

m (mol · kg ⁻¹)	$T = 288.15$ K		$T = 293.15$ K		$T = 298.15$ K		$T = 303.15$ K		$T = 308.15$ K	
	d (g · cm ⁻³)	u (m · s ⁻¹)	d (g · cm ⁻³)	u (m · s ⁻¹)	d (g · cm ⁻³)	u (m · s ⁻¹)	d (g · cm ⁻³)	u (m · s ⁻¹)	d (g · cm ⁻³)	u (m · s ⁻¹)
MeCN (1) + [C ₃ mim][Br] (2)										
0.0000	0.787376	1319.14	0.782007	1299.01	0.777609	1278.77	0.771183	1258.51	0.765725	1238.40
0.0204	0.788991	1320.25	0.783623	1300.10	0.778237	1279.97	0.772813	1259.67	0.767370	1239.62
0.0299	0.789726	1320.51	0.784364	1300.31	0.778979	1280.17	0.773562	1260.03	0.768119	1240.08
0.0404	0.790532	1321.07	0.785181	1301.12	0.779798	1281.00	0.774387	1260.87	0.768949	1240.79
0.0526	0.791470	1321.50	0.786115	1301.34	0.780735	1281.20	0.775331	1261.14	0.769896	1241.22
0.0611	0.792123	1321.96	0.786772	1301.98	0.781397	1281.87	0.775996	1261.79	0.770564	1241.73
0.0796	0.793533	1322.59	0.788186	1302.46	0.782814	1282.36	0.777417	1262.34	0.771996	1242.45
0.1027	0.795242	1323.52	0.789902	1303.43	0.784538	1283.37	0.779149	1263.39	0.773734	1243.54
0.1256	0.796939	1324.42	0.791606	1304.34	0.786248	1284.33	0.780864	1264.39	0.775460	1244.56
0.1496	0.798688	1325.32	0.793361	1305.29	0.788011	1285.31	0.782637	1265.38	0.777238	1245.61
0.1753	0.800578	1326.40	0.795262	1306.55	0.789919	1286.59	0.784553	1266.67	0.779160	1246.79
0.2069	0.802812	1327.35	0.797500	1307.38	0.792166	1287.47	0.786808	1267.64	0.781426	1247.96
0.2527	0.806071	1329.07	0.800772	1309.30	0.795452	1289.44	0.790107	1269.61	0.784738	1249.83
0.3139	0.810335	1330.95	0.805049	1311.13	0.799743	1291.33	0.794412	1271.62	0.789059	1252.07
[C ₃ mim][Br]	1.323470	1699.30	1.319844	1685.03	1.316223	1672.04	1.312600	1659.90	1.308975	1648.33
DMF (1) + [C ₃ mim][Br] (2)										
0.0000	0.953442	1496.60	0.948685	1477.27	0.943917	1457.81	0.939142	1438.38	0.934357	1419.04
0.0295	0.955471	1498.44	0.950721	1479.23	0.945962	1459.82	0.941197	1440.48	0.936424	1421.19
0.0358	0.955896	1498.74	0.951148	1479.51	0.946392	1460.11	0.941628	1440.79	0.936859	1421.49
0.0497	0.956834	1499.53	0.952089	1480.17	0.947339	1460.80	0.942580	1441.44	0.937812	1422.18
0.0591	0.957413	1499.80	0.952669	1480.29	0.947920	1460.90	0.943162	1441.61	0.938398	1422.45

Table 2 continued

<i>m</i> (mol · kg ⁻¹)	<i>T</i> = 288.15 K		<i>T</i> = 293.15 K		<i>T</i> = 298.15 K		<i>T</i> = 303.15 K		<i>T</i> = 308.15 K	
	<i>d</i> (g · cm ⁻³)	<i>u</i> (m · s ⁻¹)	<i>d</i> (g · cm ⁻³)	<i>u</i> (m · s ⁻¹)	<i>d</i> (g · cm ⁻³)	<i>u</i> (m · s ⁻¹)	<i>d</i> (g · cm ⁻³)	<i>u</i> (m · s ⁻¹)	<i>d</i> (g · cm ⁻³)	<i>u</i> (m · s ⁻¹)
0.0801	0.958776	1500.84	0.954039	1481.59	0.949295	1462.19	0.944542	1442.92	0.939782	1423.69
0.1018	0.960154	1501.65	0.955416	1482.21	0.950675	1462.88	0.945932	1443.63	0.941175	1424.51
0.1244	0.961605	1502.70	0.956878	1483.53	0.952144	1464.24	0.947403	1444.99	0.942652	1425.82
0.1525	0.963324	1503.73	0.958602	1484.40	0.953872	1465.10	0.949136	1445.92	0.944395	1426.91
0.1759	0.964790	1504.80	0.960068	1485.44	0.955349	1466.20	0.950617	1447.05	0.945882	1428.11
0.2058	0.966570	1505.78	0.961858	1486.49	0.957139	1467.29	0.952415	1448.16	0.947684	1429.18
0.2585	0.969758	1507.84	0.965060	1488.80	0.960356	1469.65	0.955641	1450.55	0.950923	1431.56
0.3035	0.972333	1509.26	0.967639	1490.09	0.962940	1470.97	0.958234	1451.96	0.955523	1433.10
[C ₃ mim][Br]	1.323470	1699.30	1.319844	1685.03	1.316223	1672.04	1.312600	1659.90	1.308975	1648.33
DMSO (1) + [C ₃ mim][Br] (2)										
0.0000	1.105336	1519.12	1.100306	1502.19	1.095278	1485.21	1.090253	1468.32	1.085231	1451.47
0.0380	1.107073	1520.94	1.102058	1504.17	1.097047	1487.28	1.092039	1470.41	1.087033	1453.62
0.0501	1.107623	1521.50	1.102611	1504.70	1.097603	1487.78	1.092600	1470.93	1.087600	1454.16
0.0594	1.108045	1521.87	1.103040	1505.18	1.098036	1488.28	1.093034	1471.43	1.088033	1454.71
0.0788	1.108910	1523.00	1.103907	1506.00	1.098912	1489.16	1.093917	1472.33	1.088929	1455.72
0.1011	1.109879	1523.78	1.104885	1507.04	1.099893	1490.21	1.094907	1473.38	1.089926	1456.68
0.1261	1.110967	1524.81	1.105976	1507.80	1.100993	1490.97	1.096017	1474.22	1.091044	1457.64
0.1490	1.111952	1525.76	1.106976	1509.09	1.102003	1492.31	1.097033	1475.55	1.092065	1458.86
0.1799	1.113266	1527.05	1.108298	1510.38	1.103331	1493.60	1.098374	1476.86	1.093417	1460.27
0.2152	1.114736	1528.50	1.109775	1511.62	1.104820	1494.86	1.099870	1478.20	1.094928	1461.69
0.2578	1.116492	1530.18	1.111547	1513.54	1.106603	1496.88	1.101667	1480.18	1.096735	1463.63
0.3109	1.118621	1532.12	1.113688	1515.32	1.108760	1498.68	1.103839	1482.06	1.098928	1465.69
[C ₃ mim][Br]	1.323470	1699.30	1.319844	1685.03	1.316223	1672.04	1.312600	1659.90	1.308975	1648.33

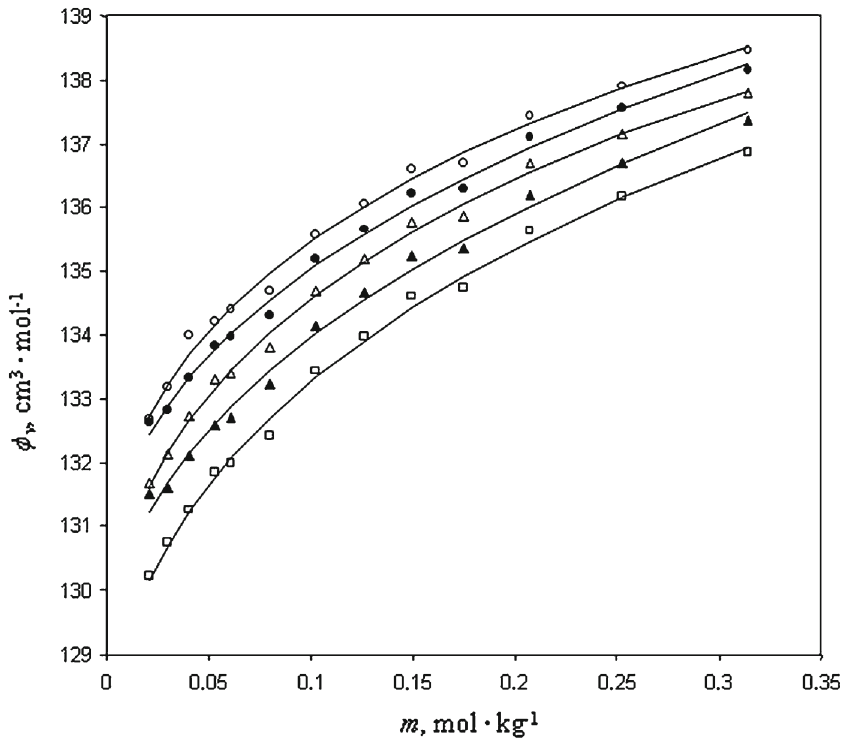


Fig. 1 Apparent molar volume of $[\text{C}_3\text{mim}][\text{Br}]$ in MeCN, ϕ_V , versus molality of $[\text{C}_3\text{mim}][\text{Br}]$, m : \circ 288.15 K, \bullet 293.15 K, \triangle 298.15 K, \blacktriangle 303.15 K, \square 308.15 K

behavior with systems investigated in this study, the speed of sound of aqueous solutions of $[\text{C}_3\text{mim}][\text{Br}]$ increases with increasing temperature and IL concentration [31].

The apparent molar volumes (ϕ_V) for $[\text{C}_3\text{mim}][\text{Br}]$ were calculated from density data by using the equation,

$$\phi_V = \frac{M}{d} + \frac{1000(d_0 - d)}{md_0d} \quad (1)$$

where M and m are the molar mass and the molality, respectively, of the IL; and d and d_0 are the densities of solutions and pure water, respectively. As examples, in Figs. 1 and 2, the temperature and concentration dependencies of ϕ_V have been given for $[\text{C}_3\text{mim}][\text{Br}]$, respectively, in MeCN and DMSO. The apparent molar volume of $[\text{C}_3\text{mim}][\text{Br}]$ for all the investigated systems in this study increases with increasing IL concentration. Figures 1 and 2 show that the apparent molar volumes of $[\text{C}_3\text{mim}][\text{Br}]$ in MeCN and DMSO decrease and increase, respectively, with increasing temperature. The apparent molar volumes of $[\text{C}_3\text{mim}][\text{Br}]$ in MeOH and H_2O , respectively, decrease and increase with increasing temperature [31]. For low concentrations of the IL, the small molar volume is attributed to the strong attractive interactions due to the solvation of ions. By increasing the salt concentration, the ion–ion interaction

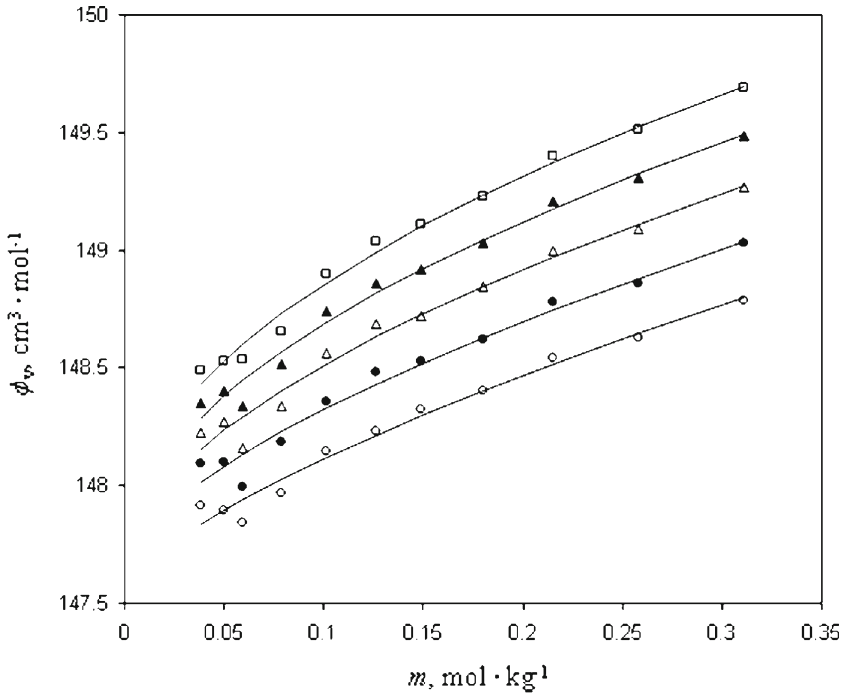


Fig. 2 Apparent molar volume of [C₃mim][Br] in DMSO, ϕ_V , versus molality of [C₃mim][Br], m : ○ 288.15 K, ● 293.15 K, △ 298.15 K, ▲ 303.15 K, □ 308.15 K

increases and the positive initial slope of ϕ_V against the IL concentration is attributed to these interactions. In the electrolyte solutions, the solute–solute interactions are characterized by positive slopes of ϕ_V versus concentration plots.

To obtain the values of the apparent molar volume data at infinite dilution, ϕ_V^0 , the values of ϕ_V obtained from Eq. 1 were fitted to a Redlich + Mayer type equation in the form,

$$\phi_V = \phi_V^0 + S_V m^{0.5} + B_V m \tag{2}$$

In this equation, S_V and B_V are the empirical parameters which depend on the solute, solvent, and temperature. The coefficients of this equation and the corresponding absolute relative deviations for ϕ_V are given in Table 3. As can be seen from Table 3, with increasing temperature, the values of ϕ_V^0 for DMF + [C₃mim][Br] and MeCN + [C₃mim][Br] systems decrease and for DMSO + [C₃mim][Br] system increase. As can be seen from Fig. 3, the ϕ_V values for DMSO mixtures are larger than those for the DMF mixtures which, in turn, are larger than those for the MeCN mixtures. In fact, as can be seen from Fig. 3, the apparent molar volume of [C₃mim][Br] in different solvents follows the order H₂O [31] > DMSO > DMF > MeOH [31] > MeCN.

The widely accepted interpretation of the infinite dilution apparent molar volume of a solute is based on the following expression:

Table 3 Fitting parameters of Eqs. 2 and 9 along with the corresponding absolute relative deviation, ARD, for the investigated systems at different temperatures T

T (K)	ϕ_V^0 ($\text{cm}^3 \cdot \text{mol}^{-1}$)	δ_V ($\text{cm}^3 \cdot \text{mol}^{-1.5} \cdot \text{kg}^{0.5}$)	B_V ($\text{cm}^3 \cdot \text{mol}^{-2} \cdot \text{kg}$)	ARD (%)	$10^{-5} \phi_K^0$ ($\text{cm}^3 \cdot \text{mol}^{-1} \cdot \text{TPa}^{-1}$)	$10^{-5} \delta_K$ ($\text{cm}^3 \cdot \text{mol}^{-1.5} \cdot \text{TPa}^{-1} \cdot \text{kg}^{0.5}$)	$10^{-5} B_K$ ($\text{cm}^3 \cdot \text{mol}^{-2} \cdot \text{TPa}^{-1} \cdot \text{kg}$)	ARD (%)
MeCN + [C₃mim][Br]								
288.15	130.124	19.5042	-8.1322	0.08	-0.853	1.3863	-1.0090	-2.53
293.15	130.123	17.0075	-4.4752	0.08	-0.888	1.2046	-0.7500	-4.35
298.15	128.850	20.7979	-8.5450	0.07	-1.105	1.8292	-1.4308	-4.37
303.15	128.838	17.2942	-3.3144	0.10	-1.158	1.3995	-0.7165	-3.05
308.15	127.272	21.2816	-7.1522	0.07	-1.363	1.7823	-1.0506	-1.41
DMF + [C₃mim][Br]								
288.15	135.652	22.9186	-15.2143	0.11	-0.266	1.0569	-0.8313	32.22
293.15	135.619	23.4440	-15.6542	0.11	-0.349	1.4437	-1.3173	-22.68
298.15	135.435	24.1997	-16.0782	0.12	-0.398	1.5747	-1.4487	-34.90
303.15	135.262	24.9085	-16.4520	0.12	-0.470	1.7768	-1.6486	-137.05
308.15	134.786	27.0102	-18.5066	0.13	-0.513	1.8110	-1.6428	104.15
DMSO + [C₃mim][Br]								
288.15	147.471	1.5863	1.4282	0.02	0.194	0.0567	0.0505	1.14
293.15	147.571	2.0556	1.0351	0.03	0.140	0.2924	-0.2091	1.45
298.15	147.597	2.7457	0.4685	0.03	0.119	0.3555	-0.2690	1.84
303.15	147.644	3.2767	0.0654	0.03	0.114	0.3495	-0.2545	1.69
308.15	147.729	3.6059	-0.1381	0.02	0.099	0.3600	-0.2428	1.68

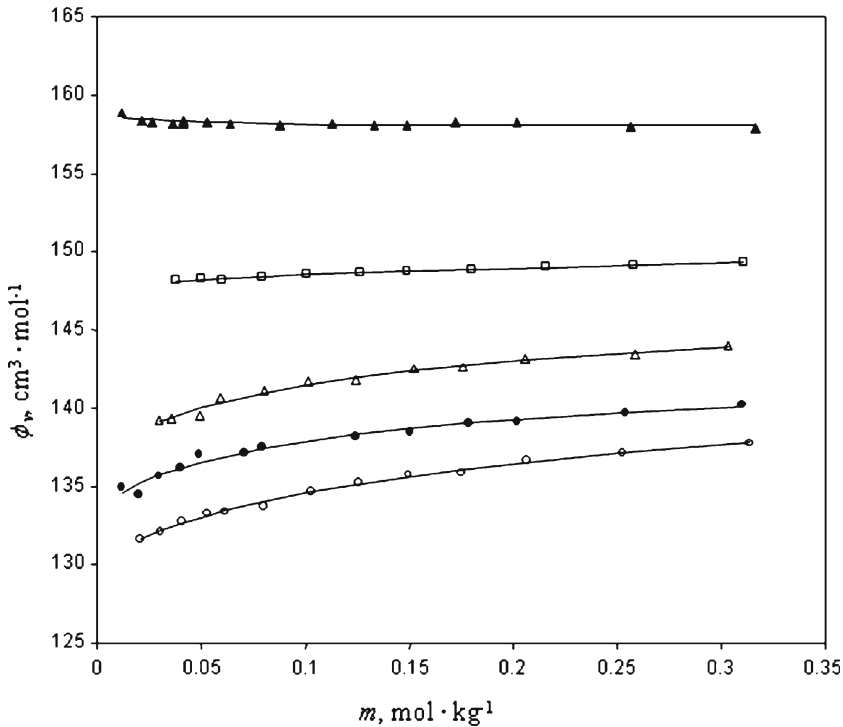


Fig. 3 Variation of the apparent molar volume, ϕ_V , at 298.15 K as a function of molality of $[\text{C}_3\text{mim}][\text{Br}]$, m , for $[\text{C}_3\text{mim}][\text{Br}]$ in: \circ MeCN, \bullet MeOH [31], \triangle DMF, \square DMSO, \blacktriangle H_2O [31]

$$\phi_V^0 = V_m^0 + \Delta V_h^0 \quad (3)$$

where V_m^0 is the intrinsic volume of the solute molecule which is inaccessible to solvent and ΔV_h^0 is the difference between the volume of the solvation shell of a solute and the volume of the bulk solvent. In other words, ΔV_h^0 is the electrostriction volume due to the solvation effects of the molecule and has a negative value. The ϕ_V^0 values reported in this study and also in Ref. [31] show that the magnitudes of ΔV_h^0 follow the order H_2O [31] < DMSO < DMF < MeOH [31] < MeCN.

Values of the excess molar volume (V^E) were calculated using the relation,

$$V^E = \sum_{j=1}^2 x_j M_j (d^{-1} - d_j^{-1}) \quad (4)$$

where M_j , x_j , d_j , and d are the molar masses of the components, mole fractions, and densities of pure liquids, and densities of mixtures, respectively, and subscript $j = 1$ is for the solvent and $j = 2$ is for $[\text{C}_3\text{mim}][\text{Br}]$. Figure 4 shows the concentration and temperature dependences of V^E for $[\text{C}_3\text{mim}][\text{Br}]$ in MeCN. From Fig. 4, it can be seen that V^E values are negative and become more negative with increasing temperature. A similar behavior has been observed for the other systems investigated in this study

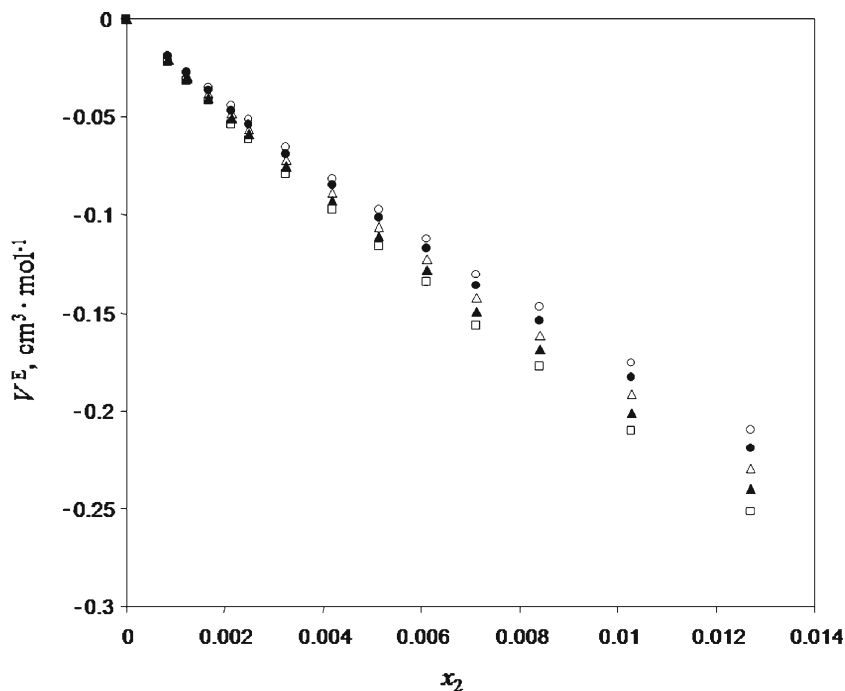


Fig. 4 Excess molar volume, V^E , versus mole fraction of $[\text{C}_3\text{mim}][\text{Br}]$, x_2 , for $\text{MeCN}(1) + [\text{C}_3\text{mim}][\text{Br}](2)$ mixture: \circ 288.15 K, \bullet 293.15 K, \triangle 298.15 K, \blacktriangle 303.15 K, \square 308.15 K

and also for methanolic solutions studied in our previous study [31]. It was found that [31] the V^E values for $[\text{C}_3\text{mim}][\text{Br}] + \text{H}_2\text{O}$ and $[\text{C}_6\text{mim}][\text{Br}] + \text{H}_2\text{O}$, are positive and negative, respectively. However, it is well known that V^E values for an IL in water become larger with increasing temperature [31,43,44]. In fact, the temperature dependence of V^E values for aqueous IL solutions is completely opposite to that for nonaqueous IL solutions. The magnitude and sign of V^E values are the result of different effects taking place in the mixture. These effects include: (a) breakdown of the solvent self-associated molecules from each other (positive volume), (b) breakdown of the IL ion-pairs (positive volume), and (c) negative contribution of volume due to the packing effect and ion–dipole interaction of solvent molecules with the IL.

The molar volume for $[\text{C}_3\text{mim}][\text{Br}]$ is $155.82 \text{ cm}^3 \cdot \text{mol}^{-1}$ at $T = 298.15 \text{ K}$, which is greater than the molar volumes of MeCN ($52.86 \text{ cm}^3 \cdot \text{mol}^{-1}$), DMF ($77.44 \text{ cm}^3 \cdot \text{mol}^{-1}$), and DMSO ($71.34 \text{ cm}^3 \cdot \text{mol}^{-1}$). The large difference between molar volumes of solvents and $[\text{C}_3\text{mim}][\text{Br}]$ implies that the relatively small solvent molecules fit in the available free volume of the IL upon mixing. The negative values of V^E for the investigated IL solutions show that the effect due to the ion–dipole interactions between $[\text{C}_3\text{mim}][\text{Br}]$ and the investigated solvents and the packing effect are dominant over the breakdown of the solvent self-associated molecules from each other and the breakdown of the IL ion-pairs.

As can be seen from Fig. 5, at $T = 298.15 \text{ K}$, the V^E values for MeCN mixtures are more negative than those for the DMF mixtures which, in turn, are more negative than

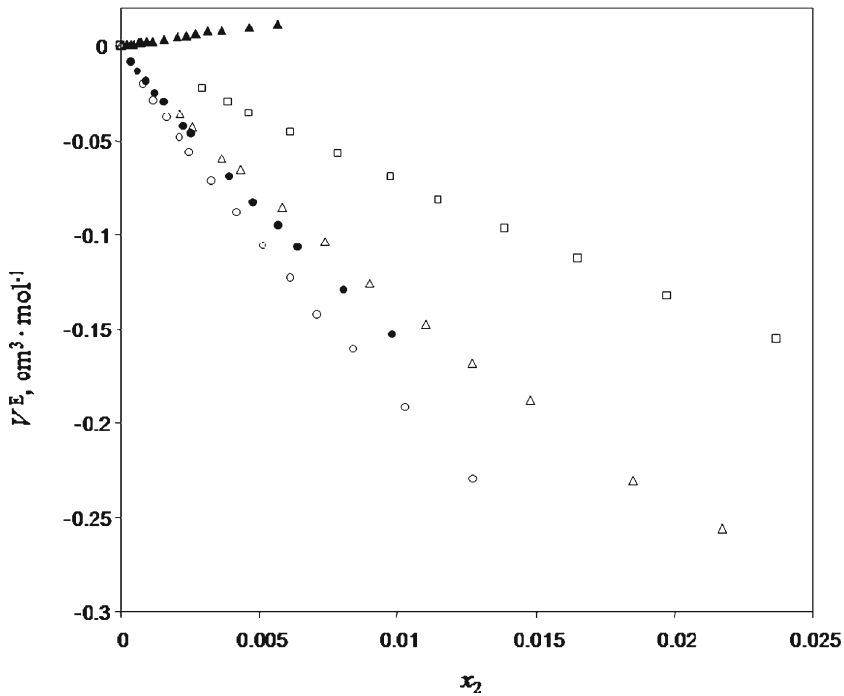


Fig. 5 Variation of the excess molar volume, V^E , at 298.15 K as a function of mole fraction of $[\text{C}_3\text{mim}][\text{Br}]$, x_2 , for $[\text{C}_3\text{mim}][\text{Br}]$ in: \circ MeCN, \bullet MeOH [31], \triangle DMF, \square DMSO, \blacktriangle H_2O [31]

those for the DMSO mixtures. Similar behavior is observed for the other isotherms. The negative values of V^E for the MeCN + $[\text{C}_3\text{mim}][\text{Br}]$ that are larger than those for the DMF + $[\text{C}_3\text{mim}][\text{Br}]$ and DMSO + $[\text{C}_3\text{mim}][\text{Br}]$ systems imply that in the MeCN solutions there are stronger ion–dipole interactions and packing effects than in the DMF and DMSO solutions. As can be seen from Fig. 5, although the molar volume of DMSO is slightly smaller than for DMF (therefore, in the DMSO solutions there are stronger packing effects than in the DMF solutions), the V^E values for DMF mixtures are more negative than for DMSO mixtures. This is because DMF has stronger ion–dipole interactions with $[\text{C}_3\text{mim}][\text{Br}]$ than does DMSO. Furthermore, the larger dielectric constant for DMSO (46.50 [45]) than for DMF (36.71 [45]) or MeCN (35.94 [45]) indicates that the effects due to the breakdown of the IL ion-pairs for DMSO solutions are larger than those for DMF or MeCN solutions. Figure 5 shows that, similar to the apparent molar volume, the excess molar volume, V^E , for $[\text{C}_3\text{mim}][\text{Br}]$ in different solvents follows the order H_2O [31] > DMSO > DMF > MeOH [31] > MeCN.

Based on the speed-of-sound and density values, the isentropic compressibility, κ_s , values were calculated for the investigated mixtures from Laplace–Newton’s equation:

$$\kappa_s = d^{-1} u^{-2} \quad (5)$$

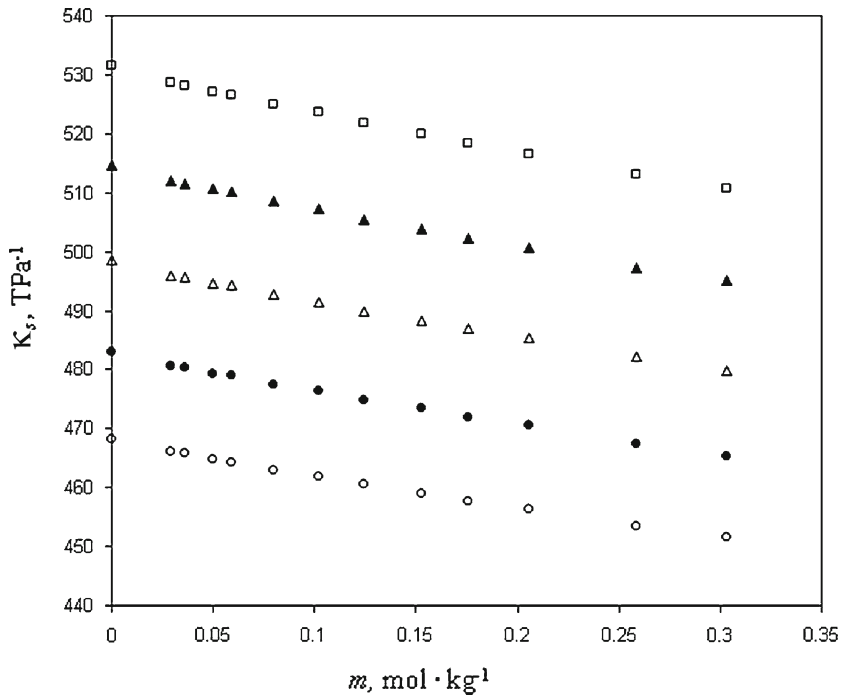


Fig. 6 Variation of isentropic compressibility, κ_s , versus molality of $[\text{C}_3\text{mim}][\text{Br}]$, m , for DMF(1) + $[\text{C}_3\text{mim}][\text{Br}]$ (2) mixture: ○ 288.15 K, ● 293.15 K, △ 298.15 K ▲ 303.15 K, □ 308.15 K

where u is the speed of sound for the investigated mixtures. The isentropic compressibility of all solutions investigated in this study (similar to the $[\text{C}_3\text{mim}][\text{Br}] + \text{MeOH}$ system [31]) decreases with increasing concentration of the IL and decreasing temperature. As an example, in Fig. 6, the temperature and concentration dependencies of κ_s have been given for $[\text{C}_3\text{mim}][\text{Br}]$ in DMF. It is well known that the isentropic compressibility of the aqueous IL solutions decreases with increasing concentration of IL and temperature. In electrolyte solutions, κ_s is the sum of two contributions, κ_s (solvent intrinsic) and κ_s (solute intrinsic). Here κ_s (solvent intrinsic) is the isentropic compressibility due to the compression of the structure of the solvent and κ_s (solute intrinsic) is the isentropic compressibility due to the compression of the solvation shell of ions and intermolecular distance of the IL chain (free volume) and also incorporation of solvent molecules into the IL chain. In fact, for the concentration range investigated in this study (very low concentrations), κ_s (solvent intrinsic) is the dominant contribution to the total value of κ_s . At the investigated temperatures, the isentropic compressibilities of all pure solvents are larger than those of the pure IL. Therefore, we may conclude that in this temperature range the compressibility of a dilute IL solution is mainly due to the effect of pressure on the bulk (unsolvated) solvent molecules.

As the concentration of the IL increases and a large portion of solvent molecules are solvated, the amount of bulk solvent decreases causing a decrease in the

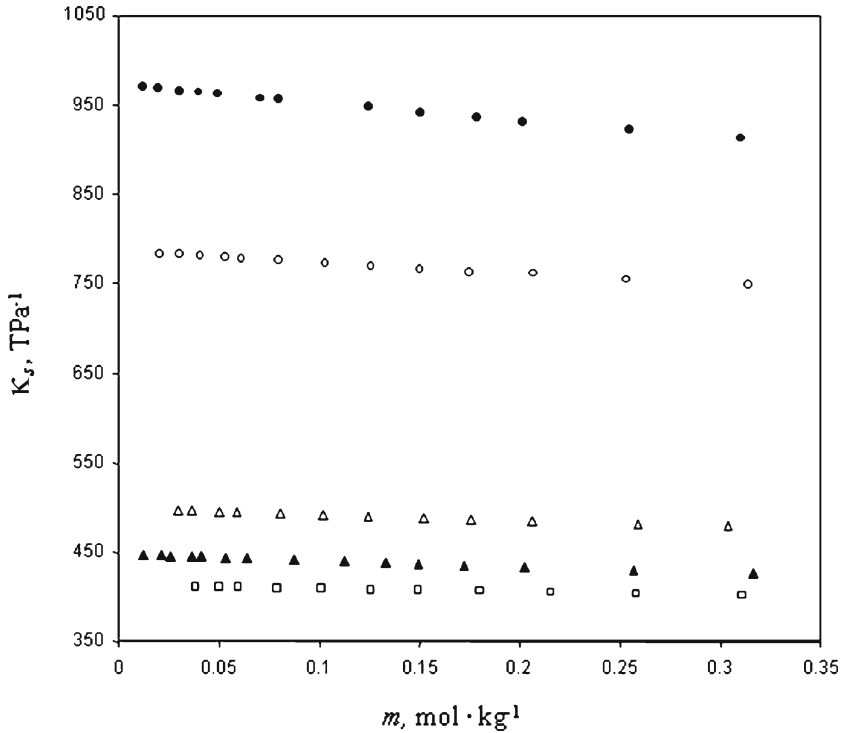


Fig. 7 Variation of isentropic compressibility, κ_s , at 298.15 K as a function of molality of $[\text{C}_3\text{mim}][\text{Br}]$, m , for $[\text{C}_3\text{mim}][\text{Br}]$ in: \circ MeCN, \bullet MeOH [31], \triangle DMF, \square DMSO, \blacktriangle H_2O [31]

compressibility. The isentropic compressibilities for both pure solvents investigated in this study and Ref. [31] (except for water) and the pure IL increase with increasing temperature. Therefore, it can be expected that the isentropic compressibility for the investigated solutions (except for aqueous solutions) increase with increasing temperature. In Fig. 7 the values of κ_s are plotted as a function of $[\text{C}_3\text{mim}][\text{Br}]$ concentration for different solvents investigated in this study along with those for water and methanol [31] at 298.15 K. Figure 7 shows that, similar to the pure solvents, the $[\text{C}_3\text{mim}][\text{Br}] + \text{MeCN}$ solutions are more compressible than the $[\text{C}_3\text{mim}][\text{Br}] + \text{DMF}$ solutions which, in turn, are slightly more compressible than the $[\text{C}_3\text{mim}][\text{Br}] + \text{DMSO}$ solutions. In fact, similar to the pure solvents, the isentropic compressibility of different IL solutions follows the order, MeOH [31] $>$ MeCN $>$ DMF $>$ H_2O [31] $>$ DMSO .

The experimental isentropic compressibility deviations, $\Delta\kappa_s$, are obtained using the relation,

$$\Delta\kappa_s = \kappa_s - \left(\sum_{j=1}^2 x_j \kappa_{sj} \right) \quad (6)$$

where κ_{sj} is the value of the isentropic compressibility of pure component j . Figure 8 shows the concentration and temperature dependencies of $\Delta\kappa_s$ for $[\text{C}_3\text{mim}][\text{Br}]$ in

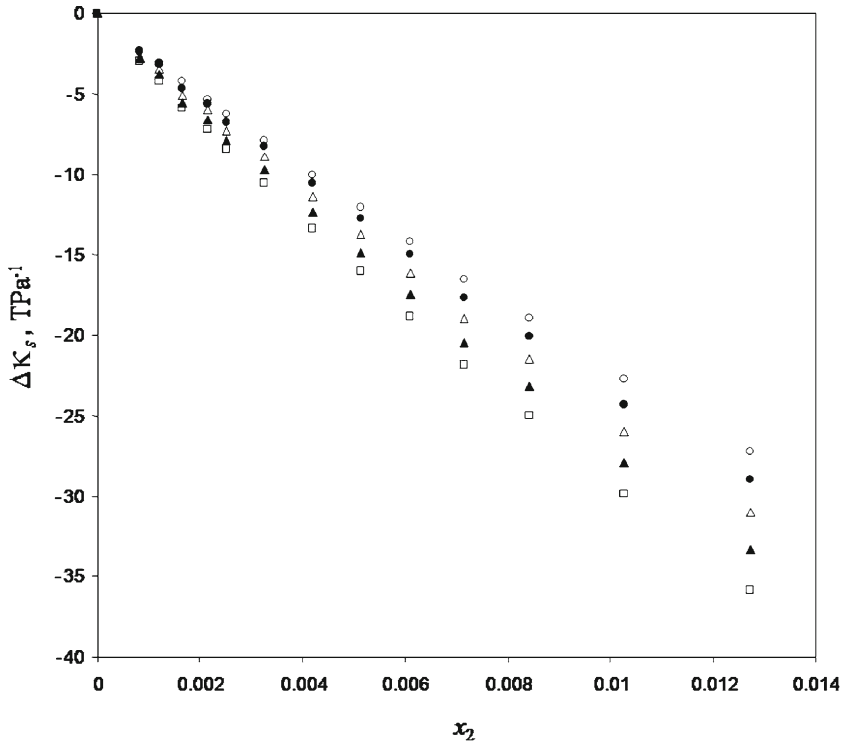


Fig. 8 Variation of isentropic compressibility deviations, $\Delta\kappa_s$, versus mole fraction of [C₃mim][Br], x_2 , for MeCN(1) + [C₃mim][Br](2) mixture: ○ 288.15 K, ● 293.15 K, △ 298.15 K, ▲ 303.15 K, □ 308.15 K

MeCN. From Fig. 8, it can be seen that the $\Delta\kappa_s$ values are negative and become more negative with increasing temperature. A similar behavior has been observed for the other systems investigated in this study. Figure 9 shows that for the systems investigated in this study, the behavior of $\Delta\kappa_s$ versus IL mole fraction is very similar to those of the excess molar volume at all studied temperatures. In fact, the $\Delta\kappa_s$ values for MeCN mixtures are more negative than those for the DMF mixtures which, in turn, are more negative than those for the DMSO mixtures.

The apparent molar isentropic compressibility ϕ_K is defined as

$$\phi_K = - \left(\frac{\partial \phi_V}{\partial P} \right)_S \quad (7)$$

The apparent molar isentropic compressibility of [C₃mim][Br], ϕ_K , in the studied solvents was computed from the density and sound-speed experimental data according to the following equation:

$$\phi_K = \frac{1000(\kappa_s - \kappa_{s0})}{md_0} + \kappa_s \phi_V \quad (8)$$

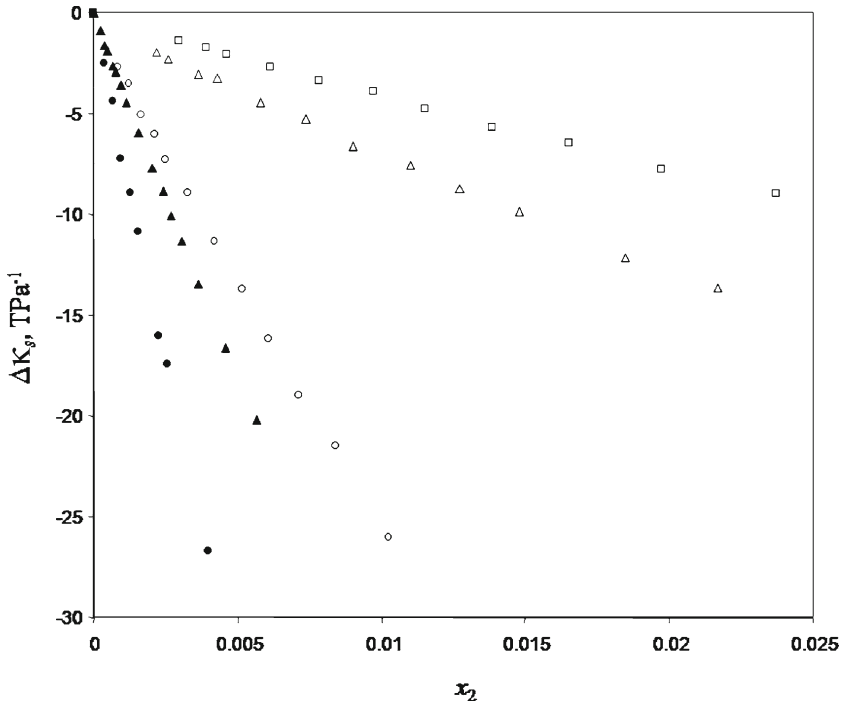


Fig. 9 Variation of isentropic compressibility deviations, $\Delta\kappa_s$, at 298.15 K as a function of mole fraction of $[\text{C}_3\text{mim}][\text{Br}]$, x_2 , for $[\text{C}_3\text{mim}][\text{Br}]$ in: \circ MeCN, \bullet MeOH [31], Δ DMF, \square DMSO, \blacktriangle H_2O [31]

where κ_s and κ_{s0} are the isentropic compressibilities of the solution and solvent, respectively. Similar to the apparent molar volume, an equation of the form,

$$\phi_K = \phi_K^0 + S_K m^{0.5} + B_K m \tag{9}$$

was used for correlating the experimental apparent molar isentropic compressibility data. Here ϕ_K^0 is the limiting apparent molar isentropic compressibility, and S_K and B_K are the empirical parameters which depend on the solute, solvent, and temperature. The coefficients of this equation and the corresponding absolute relative deviation for ϕ_K are also given in Tables 3. As an example, in Fig. 10, the temperature and concentration dependencies of ϕ_K have been given for $[\text{C}_3\text{mim}][\text{Br}]$ in MeCN. A similar behavior has been obtained for other systems studied in this work and also for the $[\text{C}_3\text{mim}][\text{Br}] + \text{MeOH}$ system [31] studied in our previous work. The apparent molar isentropic compressibility of $[\text{C}_3\text{mim}][\text{Br}]$ in water increases with an increase in temperature [31].

In Fig. 11 the effect of the type of solvent on the concentration dependence of ϕ_K has been given for $[\text{C}_3\text{mim}][\text{Br}]$ at 298.15 K. A similar behavior has been obtained for other temperatures studied in this work. The apparent molar isentropic compressibilities of $[\text{C}_3\text{mim}][\text{Br}]$ in MeCN and DMSO, respectively, have negative and positive values. The apparent molar isentropic compressibilities of $[\text{C}_3\text{mim}][\text{Br}]$ in DMF at low

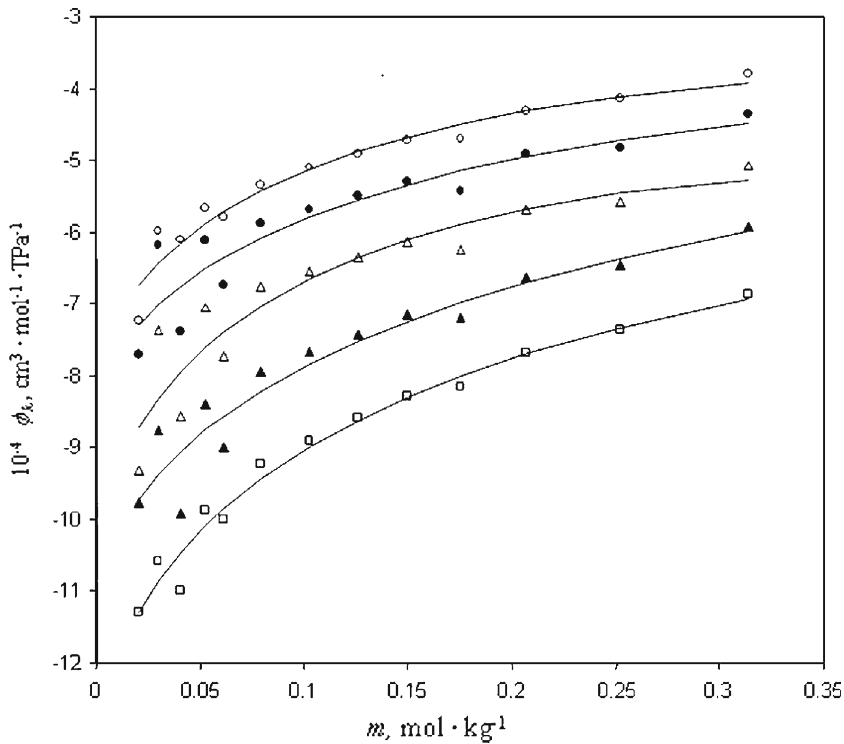


Fig. 10 Apparent molar isentropic compressibility of $[\text{C}_3\text{mim}][\text{Br}]$ in MeCN, ϕ_K , versus molality of $[\text{C}_3\text{mim}][\text{Br}]$, m : \circ 288.15 K, \bullet 293.15 K, \triangle 298.15 K, \blacktriangle 303.15 K, \square 308.15 K

IL molality have negative values; however, at high IL molality, they have positive values. For all investigated systems in this study, the values of ϕ_K increase with increasing IL molality and decreasing temperature. The negative values of the apparent molar isentropic compressibility (loss of compressibility of the medium) imply that the solvent molecules around the solute are less compressible than the solvent molecules in the bulk solutions. In fact, the negative values of ϕ_K of $[\text{C}_3\text{mim}][\text{Br}]$ in MeCN and DMF are attributed to the strong attractive interactions due to the solvation of ions in these solvents. From Eqs. 3 and 7, we obtain the following expression for the infinite dilution apparent molar isentropic compressibility of a solute:

$$\phi_K^0 = K_m^0 + \Delta K_h^0 \quad (10)$$

where K_m^0 is the intrinsic molar isentropic compressibility of the solute volume V_m^0 and ΔK_h^0 is the difference between the compressibility of the solvation shell of a solute and the compressibility of the bulk solvent.

Since the effect of pressure on the volume of crystals of low molar mass solutes which have no cavities in their structure is small, one would expect K_m^0 for low molar mass solutes to be positive and close to zero. The values of K_m^0 for high molar mass molecules are also positive, and their contribution can be significant. Therefore, the

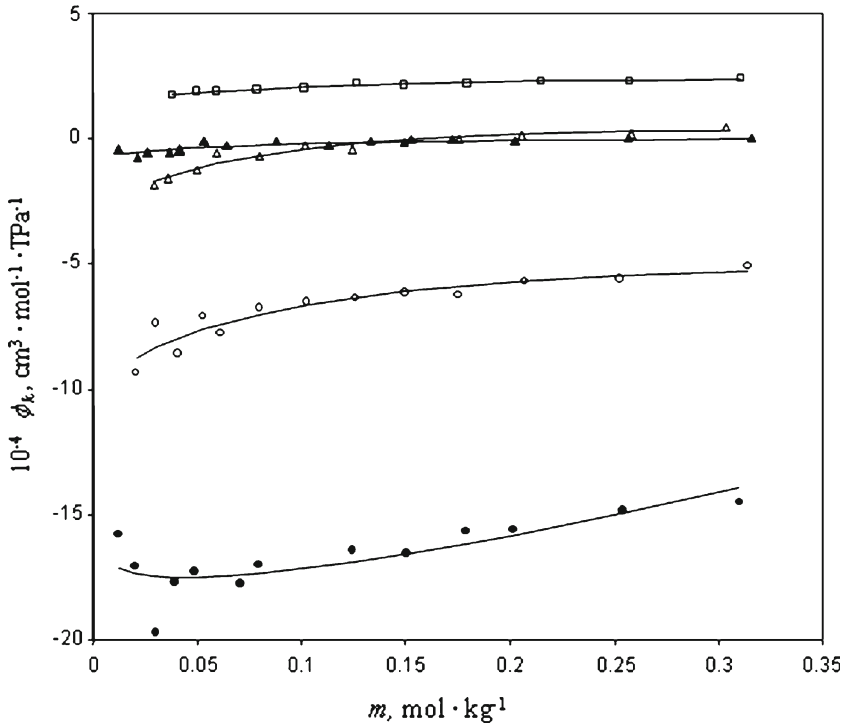


Fig. 11 The variation of the apparent molar isentropic compressibility, ϕ_K , at 298.15 K as a function of molality of $[\text{C}_3\text{mim}][\text{Br}]$, m , for $[\text{C}_3\text{mim}][\text{Br}]$ in: \circ MeCN, \bullet MeOH [31], \triangle DMF, \square DMSO, \blacktriangle H_2O [31]

bulkiness of the large hydrophobic cations of ILs suggests that their intrinsic molecular compressibilities might account for some of the apparent increase of compressibility in relation to that for small inorganic ions. The ϕ_K^0 values reported in Table 3 show that the values of ΔK_h^0 for MeCN are more negative than those for the DMF mixtures which, in turn, are more negative than those for the DMSO mixtures. This behavior indicates that in the MeCN solutions there are stronger ion–dipole interactions than in the DMF and DMSO solutions, and also the DMF–IL interactions are stronger than the DMSO–IL interactions.

4 Conclusions

Experimental data at $T = (288.15 \text{ to } 308.15) \text{ K}$ of the density and speed of sound for mixtures of $[\text{C}_3\text{mim}][\text{Br}]$ with MeCN, DMF, and DMSO have been reported. The values of excess molar volumes and isentropic compressibility deviations of solutions were calculated from the measured data. Both the excess molar volumes and the isentropic compressibility deviations are negative and become more negative as the temperature or concentration of the IL increases. When mixing $[\text{C}_3\text{mim}][\text{Br}]$ with organic solvents, we observe that the effect due to the ion–solvent interactions and

packing between organic solvents and $[\text{C}_3\text{mim}][\text{Br}]$ are dominant over the disruption of dipolar orders in organic solvents and the breakdown of the IL ion-pairs. The data presented clearly show that the magnitudes of the V^E and $\Delta\kappa_s$ values essentially follow the order $[\text{C}_3\text{mim}][\text{Br}] + \text{DMSO} > [\text{C}_3\text{mim}][\text{Br}] + \text{DMF} > [\text{C}_3\text{mim}][\text{Br}] + \text{MeCN}$, which implies that in the MeCN solutions there are stronger ion–dipole interactions and packing effects than in the DMF and DMSO solutions.

References

1. T. Welton, Chem. Rev. **99**, 2071 (1999)
2. P. Wasserscheid, W. Keim, Angew. Chem. Int. Ed. **39**, 3772 (2000)
3. P. Wasserscheid, T. Welton (eds.), *Ionic Liquids in Synthesis* (Wiley-VCH, Weinheim, 2003)
4. C. Reichardt, Org. Process Res. Dev. **11**, 105 (2007)
5. J.S. Wilkes, Green Chem. **4**, 73 (2002)
6. P. Wasserscheid, W. Keim, Angew. Chem. **112**, 3926 (2000)
7. R.D. Rogers, K.R. Seddon, *Ionic Liquids Industrial. Applications to Green Chemistry* (American Chemical Society, Washington, DC, 2002)
8. P. Bonhote, A.P. Dias, N. Papageorgiou, K. Kalyanasundaram, M. Gratzel, Inorg. Chem. **35**, 1168 (1996)
9. J.G. Huddleston, A.E. Visser, W.M. Reichert, H.D. Willauer, G.A. Broker, R.D. Rogers, Green Chem. **3**, 156 (2001)
10. Y.U. Paulechka, G.J. Kabo, A.V. Blokhin, A.S. Shaplov, E.I. Lozinskaya, S.Y. Vegodskii, J. Chem. Thermodyn. **39**, 158 (2007)
11. G. Law, P.R. Watson, Langmuir **17**, 6138 (2001)
12. H.L. Ngo, K. LeCompte, L. Hargens, A.B. McEwen, Thermochim. Acta. **357**, 97 (2000)
13. K.S. Kim, B.K. Shin, F. Ziegler, Fluid Phase Equilib. **218**, 215 (2004)
14. J.M. Crosthwaite, M.J. Muldoon, J.K. Dixon, J.L. Anderson, J.F. Brennecke, J. Chem. Thermodyn. **37**, 559 (2005)
15. R.M. Diamond, J. Phys. Chem. **67**, 2513 (1963)
16. J. Wang, H. Wang, S. Zhang, H. Zhang, Y. Zhao, J. Phys. Chem. B **111**, 6181 (2007)
17. L. Gaillon, J. Sirieix-Plenet, P. Letellier, J. Solut. Chem. **33**, 1333 (2004)
18. M.A. Firestone, J.A. Dzielawa, P. Zapol, L.A. Curtiss, S. Seifert, M.L. Dietz, Langmuir **18**, 7258 (2002)
19. M.T. Zafarani-Moattar, H. Shekaari, J. Chem. Thermodyn. **37**, 1029 (2005)
20. I. Goodchild, L. Collier, S.L. Millar, I. Prokes, J.C.D. Lord, C.P. Butts, J. Bowers, J.R.P. Webster, R.K. Heenan, J. Colloid Interface Sci. **307**, 455 (2007)
21. R.L. Gardas, D.H. Dagade, J.A.P. Coutinho, K.J. Patil, J. Phys. Chem. B **112**, 3380 (2008)
22. H. Shekaari, Y. Mansoori, R. Sadeghi, J. Chem. Thermodyn. **40**, 852 (2008)
23. M.T. Zafarani-Moattar, S. Hamzehzadeh, J. Chem. Eng. Data **52**, 1686 (2007)
24. J. Sirieix-Plenet, L. Gaillon, P. Letellier, Talanta **63**, 979 (2004)
25. B. Dong, L. Zheng, L. Yu, T. Inoue, Langmuir **23**, 4178 (2007)
26. T. Singh, A. Kumar, J. Phys. Chem. B **111**, 7843 (2007)
27. T. Inoue, H. Ebina, B. Dong, L. Zheng, J. Colloid Interface Sci. **314**, 236 (2007)
28. R. Vanyur, L. Biczok, Z. Miskolczy, Colloids Surf. A **299**, 256 (2007)
29. U. Domanska, A. Pobudkowska, M. Rogalski, J. Colloid Interface Sci. **322**, 342 (2008)
30. B. Dong, X. Zhao, L. Zheng, J. Zhang, N. Li, T. Inoue, Colloids Surf. A **317**, 666 (2008)
31. R. Sadeghi, H. Shekaari, R. Hosseini, J. Chem. Thermodyn. **41**, 273 (2009)
32. D. Das, B. Das, D.K. Hazra, J. Mol. Liq. **111**, 15 (2004)
33. M.T. Zafarani-Moattar, H. Shekaari, J. Chem. Eng. Data **50**, 1694 (2005)
34. J.Z. Yang, J. Tong, J.B. Li, J. Solut. Chem. **36**, 573 (2007)
35. Y. Pei, J. Wang, L. Liu, K. Wu, Y. Zhao, J. Chem. Eng. Data **52**, 2026 (2007)
36. H. Shekaari, M.T. Zafarani-Moattar, Int. J. Thermophys. **29**, 534 (2008)
37. N. Saha, B. Das, D. Hazra, J. Chem. Eng. Data **40**, 1264 (1995)
38. M.G. Prolongo, R.M. Masegosa, I.H. Fuentes, A. Horta, J. Phys. Chem. **88**, 2163 (1984)
39. J. Krakowiak, D. Bobicz, W. Grzybkowski, J. Mol. Liq. **88**, 197 (2000)

40. T.M. Aminabhavi, G. Bindu, J. Chem. Eng. Data **40**, 856 (1995)
41. K. Miyai, M. Nakamura, K. Tamura, S. Murakami, J. Solut. Chem. **26**, 973 (1997)
42. J.A. Riddick, W.B. Bunger, T.Y. Sakano, *Organic Solvents*, 4th edn. (Wiley-Interscience, New York, 1986)
43. E. Gomez, B. Gonzalez, A. Dominguez, E. Tojo, J. Tojo, J. Chem. Eng. Data **51**, 696 (2006)
44. E. Vercher, A.V. Orchilles, P.J. Miguel, A. Martinez-Andreu, J. Chem. Eng. Data **52**, 1468 (2007)
45. Y. Marcus, *The Properties of Solvents* (Wiley, Chichester, 1998)